

Chapter 37

GHRM Error Sources

In This Chapter...

About Flux Calibrations / 37-2
Spectrum Level and the Sensitivity Function / 37-2
Spectrum Shape / 37-16
Spectrum Noise and Structure / 37-18
Calibration Quality Files / 37-22
About Wavelength Calibrations / 37-23
Spatial Uncertainty: Target Acquisition Problems / 37-28
Observation Timing / 37-29
Instrument and Spacecraft Errors / 37-31

A GHRM spectrum has several dimensions, each with associated error and uncertainty. The two most obvious dimensions are flux and wavelength, which we plot to show the spectrum. But time is also a dimension of the spectrum, in the sense of when the spectrum was obtained, how long the exposure lasted, and the extent of interruptions of that exposure. Spatial dimensions—the positioning of the object within the aperture—are also relevant. Finally, there are instrumental and spacecraft errors that influence the data.

In Table 37.1, we provide a summary of the accuracies you can expect from your data when you have recalibrated it with the latest **calhrs** software and the best reference files (as recommended by StarView's Best Reference File screen—see Chapter 1 in Volume 1), assuming your target acquisition was successful and appropriate for your science slit, and, for photometry, assuming a wide aperture was used. In some cases improvements can be made further by using the calibration information and post observation refinement tasks described in this Data Handbook—these cases are noted in the table.

In this chapter we will discuss each of the dimensions affecting the accuracy of your data in turn and examine what is known about them from the experience gained since the GHRM started operation.

Table 37.1: Summary of GHRS Errors and Uncertainties^a

Attribute	Accuracy	Limiting Factors
Flux, absolute	5%	Confidence in absolute flux scale
Flux, relative: same star, same wavelength	2–4% ^b	Grating at same position for all observations
Flux, relative: within an exposure	2 to 4%	2% typical, 4% worst case (G140L, 100 Å away)
Flux, relative: different setups	4%	2% typical; vignetting, sensitivity determinations
Flux, relative: pre-COSTAR	4%	Centering in LSA, poor PSF
Wavelengths, relative: within an exposure	<0.1 diode	Dispersion highly reliable
Wavelengths, absolute: default wavelength calibration	1.1 diodes	Assumes worst case from Table 37.8
Wavelengths, absolute: use of SPYBAL	0.4 diode	GIM effects and carousel uncertainty
Wavelengths, absolute: use of wavecal	0.3 diode	GIM effects

a. See page 37-17 for applicability to G270M.

b. Can vary to 4% at shortest wavelength. For side 2, can be improved by correction for time-dependent variations, as in Figure 37.3.

37.1 About Flux Calibrations

The concept we discuss here as “flux” has several components. First, is the overall level of the spectrum, or “Has the correct flux scale been applied to the observations?” Second, is the shape of the spectrum, or “Is the curve I see in the continuum real or an artifact?” Finally, there is structure in the spectrum on the scale of a diode’s width, or “Is that noise or a bad diode?” The first component has a length scale of tens to hundreds of Ångstroms and is embodied in the sensitivity function for a grating. The second component is incorporated primarily into the vignetting function, which depends on the particular setting for a grating, although other effects can contribute on this scale as well. The small-scale structure, as noted, is seen on diode-sized scales.

37.2 Spectrum Level and the Sensitivity Function

The sensitivity functions quantify the relationship between the observed flux from a point source and the count rate detected by the GHRS. For calibration purposes the fluxes of the reference stars are expressed in the cgs units traditional to astronomy: $\text{ergs cm}^{-2} \text{sec}^{-1} \text{Å}^{-1}$. Raw GHRS data have units of counts per diode per second. The sensitivity functions simply show the ratio of these quantities, with no other constants, scale factors or transformations included. The post-COSTAR sensitivity functions for all GHRS gratings are listed in Chapter 8 of the *GHRS Instrument Handbook*¹. (See *GHRS ISR 060* for the pre-COSTAR sensitiv-

ity functions.) For planning purposes, a known or estimated flux can be multiplied by the sensitivity to estimate what the GHRS count rate will be for a particular grating. During data reduction, an observed count rate can be divided by the sensitivity function to calibrate the data in flux units by setting the value of the FLX_CORR switch to PERFORM in the .d0h header.

The sensitivity functions depend on several factors. The telescope contributes its unobscured geometrical collecting area, the reflectivity of both mirrors, and the fraction of the light which manages to pass through the instrument's entrance aperture. The GHRS optics introduce a finite reflectivity at each surface and transmission at each filter and window, the blaze efficiency and linear dispersion of the gratings. The detectors have an overall quantum efficiency (QE) at each wavelength, spatial gradients related to vignetting or real QE variations, isolated scratches and blemishes, pixel-scale irregularities, finite sampling by the diodes, and diode-to-diode gain variations. As we noted, to simplify this problem, the calibration is broken into several components. The basic function relates flux and count rate measured at the center of the diode array, for a star centered in the LSA, at a range of wavelengths for each grating. The echelle blaze function is quantified separately for each order. Gradients of sensitivity across the diode array are described by vignetting functions which vary with wavelength for each grating or echelle order. The SSA throughput is measured relative to the LSA at several wavelengths, and is assumed to be independent of grating mode. Blemishes are tabulated as departures from the local sensitivity for each grating. Diode response functions are tabulated as detector properties, which depend on threshold settings, but not optical modes. Finally, the pixel to pixel granularity can be identified and suppressed as photometric noise.

Each of these factors that affects the flux measurement has some uncertainty, which we will discuss below.

37.2.1 Standard Stars

The stars used for flux references are members of the set of standards established and maintained by STScI. Targets for specific observations are selected primarily on the basis of UV brightness and nonvariability, since we want to obtain count rates high enough to achieve adequate S/N (>50) in short exposure times.

We used the ultraviolet standard stars BD+28D4211 and μ Columbae as our primary flux references. We have also used BD+75D325 and AGK+81D266 on occasion. None of these are known to exhibit significant variability in the ultraviolet. BD+28D4211 is a hot white dwarf that was used for the sensitivity monitors for the low- and medium-dispersion gratings. The corresponding observations for the echelle, and other long-term monitoring programs, were done with the bright late-O super giant μ Col. An example of a Cycle 4 BD+28D4211 observation is in Figure 37.1.

1. The values in the *GHRS Instrument Handbook* were for purposes of observation planning and are not the final nor best information available. The CDBS files are up-to-date and based on our cumulative experience since launch.

Sensitivity determination is done by comparing an observed spectrum to the reference spectrum for that star. The reference spectrum is the current best estimate of the true flux versus wavelength for a particular star, and therefore represents “truth.” The flux scale for the GHRS and other HST instruments has been modified such that observations of the star G191B2B match theoretical models.

37.2.2 Procedures for Determining Sensitivity and Vignetting Functions

A series of observations for the characterization of the post-COSTAR GHRS was made shortly after SMOV, in 1994. A similar series was done early after launch for the pre-COSTAR instrument. To illustrate how these observations were used to determine sensitivity and vignetting, we borrow from *GHRS ISR 085*, which discusses G140L sensitivity.

If it were possible to record the full useful wavelength range of a grating in a single exposure, then it would also be possible to determine a single “sensitivity function” for that grating. That function, which we will denote by S_λ , would have units of flux per count rate², or, more physically, S_λ is in units of ($\text{erg cm}^{-2} \text{s}^{-1} \text{\AA}^{-1}$) per ($\text{counts s}^{-1} \text{diode}^{-1}$), where knowledge of the instrument’s properties indicates the appropriate wavelength at a given diode. We will denote the flux by F_λ and the count rate by C_λ , so that $S_\lambda = F_\lambda/C_\lambda$.

The work would be much easier if we could observe a “perfect” star, by which we mean one with a flat or nearly-flat spectrum which is not variable in time and which is largely free of any structure (such as absorption lines). We also wish we had a “perfect” detector to work with, which would be one with a flat response across its face, that response being independent of wavelength, spatial position, or time.

Real stars, in particular those used as standards for UV flux calibration, have many spectrum features, and those lie at astrophysically-critical wavelengths. The biggest of these, like Lyman- α , are “potholes” in that they must be worked around carefully. There are also weaker features—the “barbs”—that make it difficult to divide one spectrum by another. Real detectors, like those in the GHRS, have response functions that vary with wavelength, and, to some degree, with time. What is particularly difficult to treat is the very steep decline in sensitivity below Lyman- α .

The gratings of the GHRS can be positioned to almost any wavelength within their nominal ranges. When this is done, other effects must be taken into account. In particular, GHRS spectra have a *vignetting* correction applied after the initial sensitivity calibration. This vignetting is only partially so in the classic optical sense, and, in fact, includes several effects that lead to variations in the spectrum of a few percent over scales of tens of pixels. “Sensitivity,” on the other hand, is meant to refer to the gross dependence of observed count rate on stellar flux. Thus “sensitivity” should not depend on how a spectrum is placed on the detector; those

2. More properly this is the inverse sensitivity. We will ignore the distinction here.

spatially-dependent effects come under “vignetting.” Variations on even finer scales also occur and have to do with diode-to-diode gain variations, granularity, etc. Those small-scale (one to a few diodes in scale) variations will not be treated here.

The underlying concepts used to determine S and separate it from V , the vignetting function are simple:

1. Observe a standard star over the full useful range of the grating, ensuring that any given wavelength is observed twice by stepping the grating by half its bandwidth. This produces the observed standard star spectrum, in count rate units, $C_\lambda(O)$, as a function of wavelength.
2. Plot these overlapping spectra in the units they are observed (count rate) versus wavelength. The central region of each spectrum should form an upper envelope to what is seen.
3. Compare this upper envelope to a reference flux spectrum for the standard star, $F_\lambda(R)$. The reference spectrum is the official version of what the flux at each wavelength of the standard star is supposed to be.
4. The initial estimate of sensitivity is then $S_1 = F_\lambda(R)/C_\lambda(O)$.
5. Use this initial estimate S_1 to derive deviations for each individual spectrum. These are V_1 , determined as a function of position on the detector photocathode, the detector being the presumed source of the variations ascribed to vignetting.
6. Iterate S and V until satisfactory closure occurs, to get S_{final} and V_{final} . The goal is to determine vignetting to within about 1%.

In practice, of course, determining S_λ and V_λ is not so simple, and involves some estimates and compromises. For example, we accepted the existing CDBS G140L vignetting files as final versions and did not rederive the vignetting: the residuals in overlapping areas of the spectra were within acceptable limits.

Figure 37.1 shows the first step in this process. The upper frame shows the observed spectrum, $C_\lambda(O)$, of standard star BD+28 in units of count rate, while the bottom frame shows the reference spectrum, $F_\lambda(R)$. Please note that this reference spectrum already takes into account the proper white dwarf flux scale, and that no secondary correction is needed.

Problems and Limitations

The procedure outlined above quickly produces satisfactory results. There remain, however, some difficult nagging problems.

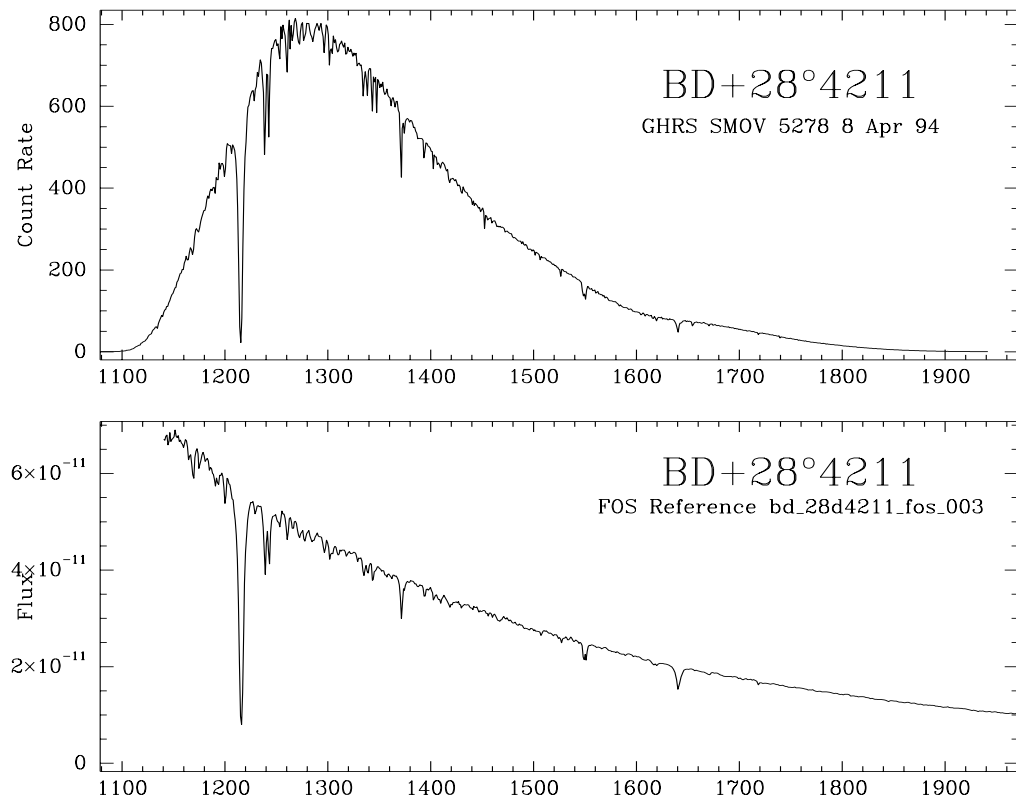
Far-UV Reference Fluxes

The existing reference spectrum of our standard star, BD+28°4211 is based on FOS observations, and are on the fundamental UV scale of G191-B2B. However, the GHRS can observe further into the UV than can the FOS, which means that we lack a reference spectrum below about 1140 Å.

Lyman- α and Other Major Features

It is difficult to determine the calibration in the region of Lyman- α because it is such a large feature. Also, Lyman- α lies on a portion of the observed spectrum with a steep slope (Figure 37.1). Lyman- α is very broad, and, moreover, there is little spectrum left shortward of Lyman- α , and the sensitivity there is declining rapidly. As a result the intrinsic uncertainty in fluxes in the region of Lyman- α is higher than at other wavelengths.

Figure 37.1: Observed Spectrum $C_\lambda(O)$ of Standard Star BD+28 (above) Compared to Reference Spectrum $F_\lambda(R)$ for the Star (below).



Various features show up in all parts of the spectrum of the standard star, but they are moderate in effect, making it possible to form a reliable estimate of the spectrum. Recall that the reference spectrum is defined in terms of the total stellar flux within some bandpass, meaning that it is *not* the flux in the continuum. The reference spectrum has its origins in FOS observations, at resolution lower than those of the GHRS. Therefore we interpolate both spectra to get the resolution of the GHRS spectra to a level similar to that of the reference spectrum.

Small Science Aperture (SSA)

The amount of light seen through the Small Science Aperture (SSA) is sensitive to the centering of the object in the SSA. The baseline SSA sensitivity curve was created by multiplying the baseline LSA sensitivity curve by the SSA to LSA ratio. The process used is discussed in greater detail later in this document.

Effects of Time

Ratios of our regular sensitivity monitoring data to the baseline SMOV data show changes in GHRS Side 1 sensitivity over time since the installation of COSTAR. Each time the monitor was run, the current data was compared to the SMOV BD+28D4211 data at the same wavelength. A ratio and errors were calculated every 10 Å from ~1100 Å to ~1630 Å. While the sensitivity below Lyman- α decreased, an apparent increase occurred in sensitivity from ~1200 to 1350 Å, before it declined again. We do not understand this behavior, but it has remained fairly constant with time.

In addition to rederiving the baseline post-COSTAR sensitivity, we have also created time-dependent curves for the date of each sensitivity monitor based on the ratio of the counts from the monitor to the SMOV baseline data. Observers will need to interpolate between sensitivity curves to get a correction appropriate for the date of their observations.

37.2.3 Sensitivity Monitoring

Sensitivity monitoring was done for Side 1 and Side 2 separately. The Side 1 post-COSTAR monitor contained a series of visits of the ultraviolet standard BD+28D4211, done with identical instrumental configuration each time, except that the exposure times were increased at later dates to achieve better signal to noise. The target was acquired into the Large Science Aperture with a 5 x 5 spiral search using mirror N1, followed by a peak-up. The science observations were done with grating G140L in the ACCUM mode at two central wavelengths: 1200 Å and 1500 Å. For the Side 2 observations, BD+28D4211 was acquired into the LSA with a 3 x 3 spiral search using mirror N2, followed by a peak-up. Centering was confirmed by taking an image with the LSA. A series of spectra in the ACCUM mode were taken with gratings G160M (centered at 1200 and 1500 Å), G200M (2000 Å), and G270M (2500 and 3000 Å). This sequence was repeated approximately every three months.

These monitoring programs have shown that prior to COSTAR and the 1993 Servicing Mission, the GHRS was stable in sensitivity, with no perceptible changes. However, after the Servicing Mission we could see distinct declines in sensitivity, especially on Side 1 below Lyman- α . These changes were suspected to be due to contamination on the COSTAR mirrors for the GHRS, and a special measurement was planned to occur just before the second Servicing Mission to verify this. Unfortunately, the GHRS experienced a catastrophic failure one week before SM2 so that these measurements were never done.

In any case, the declines in the post-COSTAR sensitivity of the GHRS are well-characterized. Typical errors in the ratios are less than 1% for wavelengths above 1200 Å and around 1 to 2% for wavelengths below 1200 Å (up to 3 to 4% on the 1100 Å point at the earliest dates with the least exposure time). Provision has been made for the decline by providing calibration reference files that apply to specific time periods. These time periods are three months in length, which is short enough that significant changes did not occur on shorter time scales. The difference between successive sensitivity files is listed in Table 37.2 below.

Table 37.2: Differences between Successive G140L Time Dependent Sensitivities

USEAFTER	MEAN	STDDEV	100x(1-MIN)	100x(1-MAX)
June 14, 1994	1.0133	0.0414573	1.41860	-14.449
August 1, 1994	1.00233	0.0087619	0.5979	-2.727
October 21, 1994	0.995793	0.0086304	1.2088	-1.443
January 14, 1995	1.01144	0.019553	0.0589	-7.321
April 17, 1995	1.02364	0.0254328	0.1453	-10.448
June 25, 1995	0.995898	0.0068702	2.2658	-0.814
September 17, 1995	0.994218	0.0213934	6.7518	-1.19
January 4, 1996	1.01534	0.0274196	-0.0120	-9.668
May 2, 1996	0.997726	0.0093042	2.40010	-0.524
August 30, 1996	1.00581	0.00362	0.23299	-1.263
November 22, 1996	1.01707	0.0345412	0.80189	-12.303
January 24, 1997	0.996619	0.0109268	1.40099	-2.483

Figure 37.2 shows the Side 1 sensitivity decline and Figure 37.3 shows the decline for Side 2. The Side 1 figure represents fits to the sensitivity monitor ratios for grating G140L. Illustrated are cubic-spline fits to the ratios of an observed spectrum to the one observed during SMOV. These fits are the basis for the time-variable G140L sensitivity files. Figure 37.4 and Figure 37.5 show details of the time variability for the two worst wavelength regions.

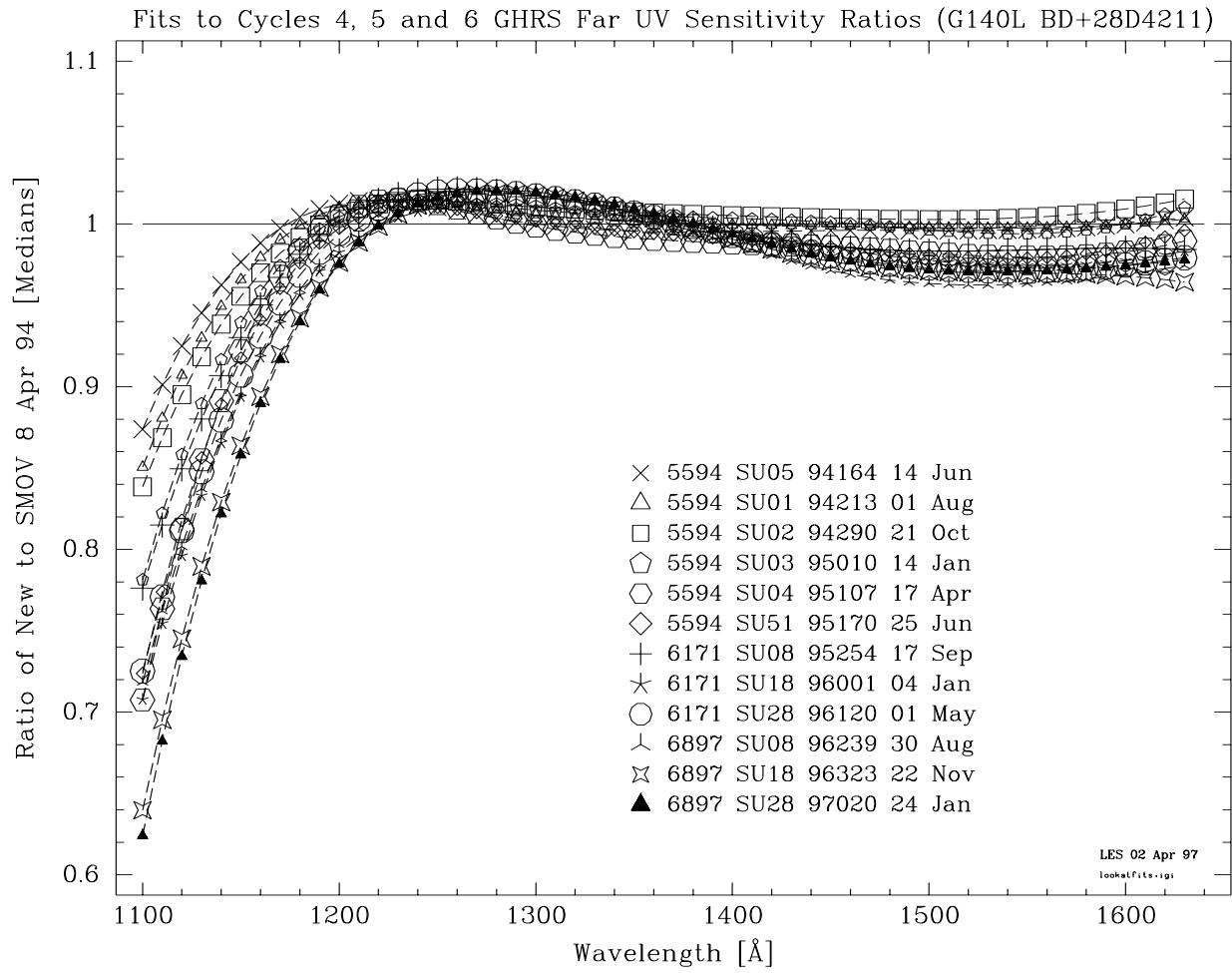
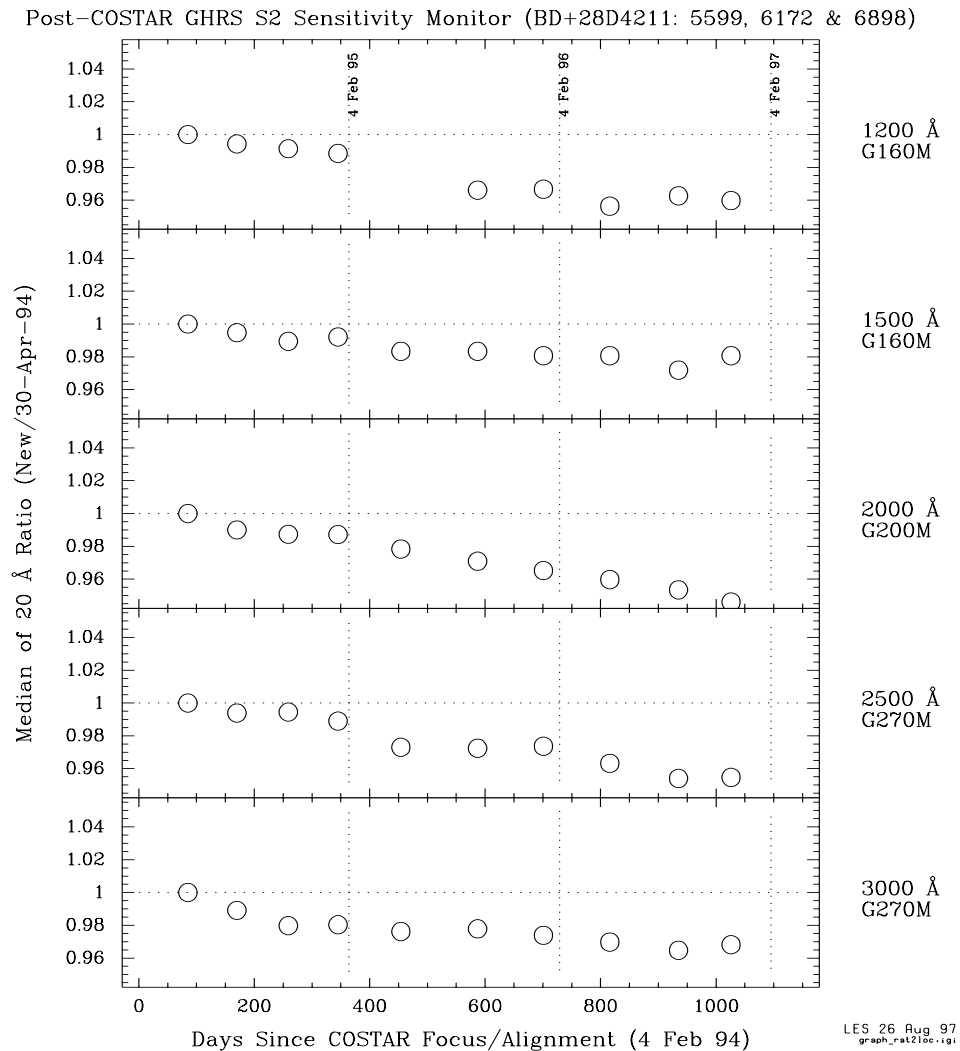
Figure 37.2: Side 1 Sensitivity Decline

Figure 37.3: Side 2 Sensitivity Since COSTAR

In Figure 37.3, the five panels are for central wavelengths of 1200 Å, 1500 Å, 2000 Å, 2500 Å, and 3000 Å. Each point represents the ratio of the median counts measured over 20 Å relative to the counts measured on 30 April 1994 over the same 20 Å (the first data point). The error on individual data points is 1%. Time is represented in days using the date we consider COSTAR to have aligned and focussed for GHRS (February 4, 1994) as the zero-point. The vertical dashed lines represent one-year intervals.

An example of the improvement possible from using the time-dependent files is shown in Figure 37.6. In this figure, the top plot is flux-corrected with an appropriate time-variable sensitivity file; the bottom plot is the same data calibrated by the pipeline (PODPS).

Figure 37.4: Time Variability for GHRS G140L Below Ly- α

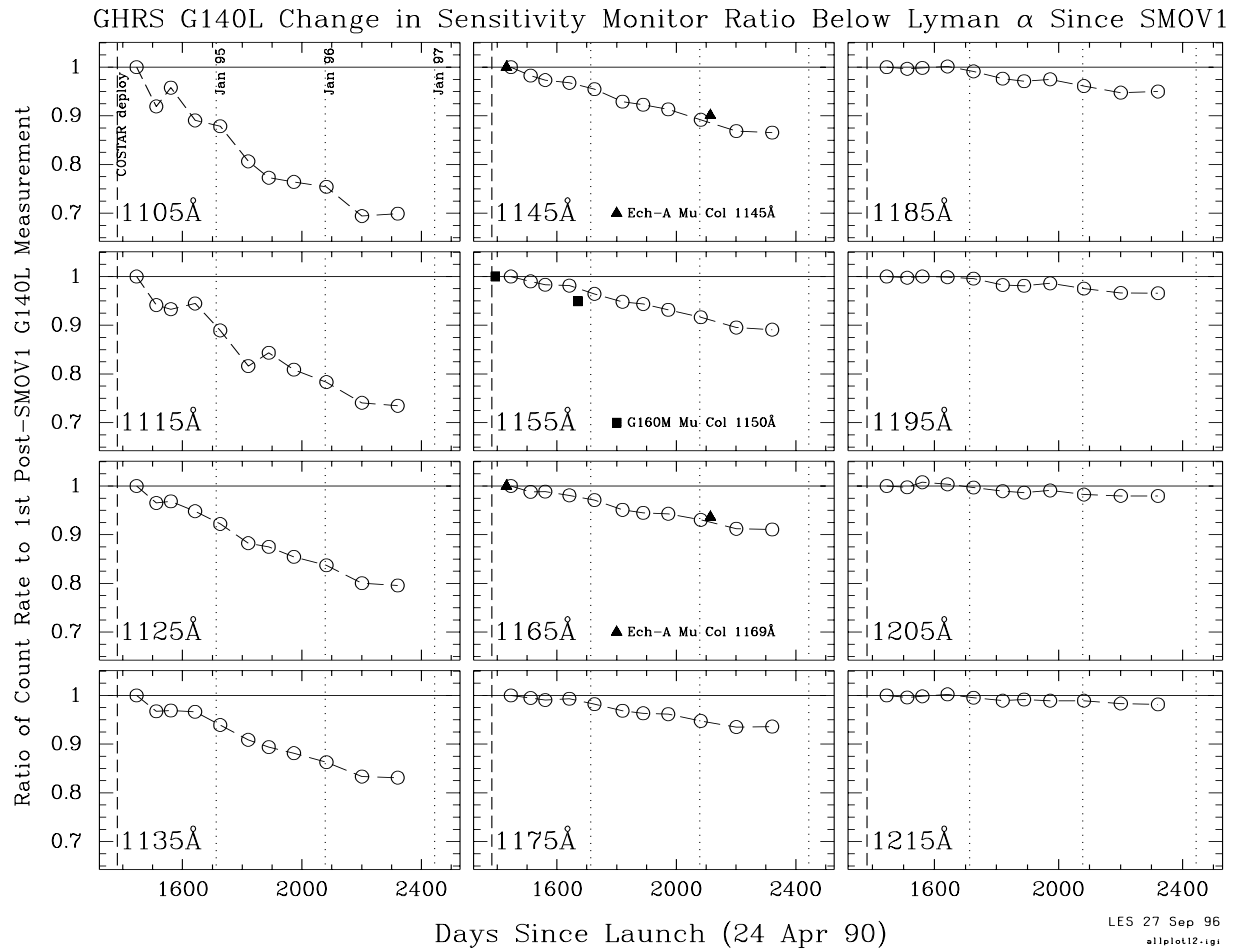


Figure 37.5: GHRs G140L Change in Sensitivity Monitor Ratio

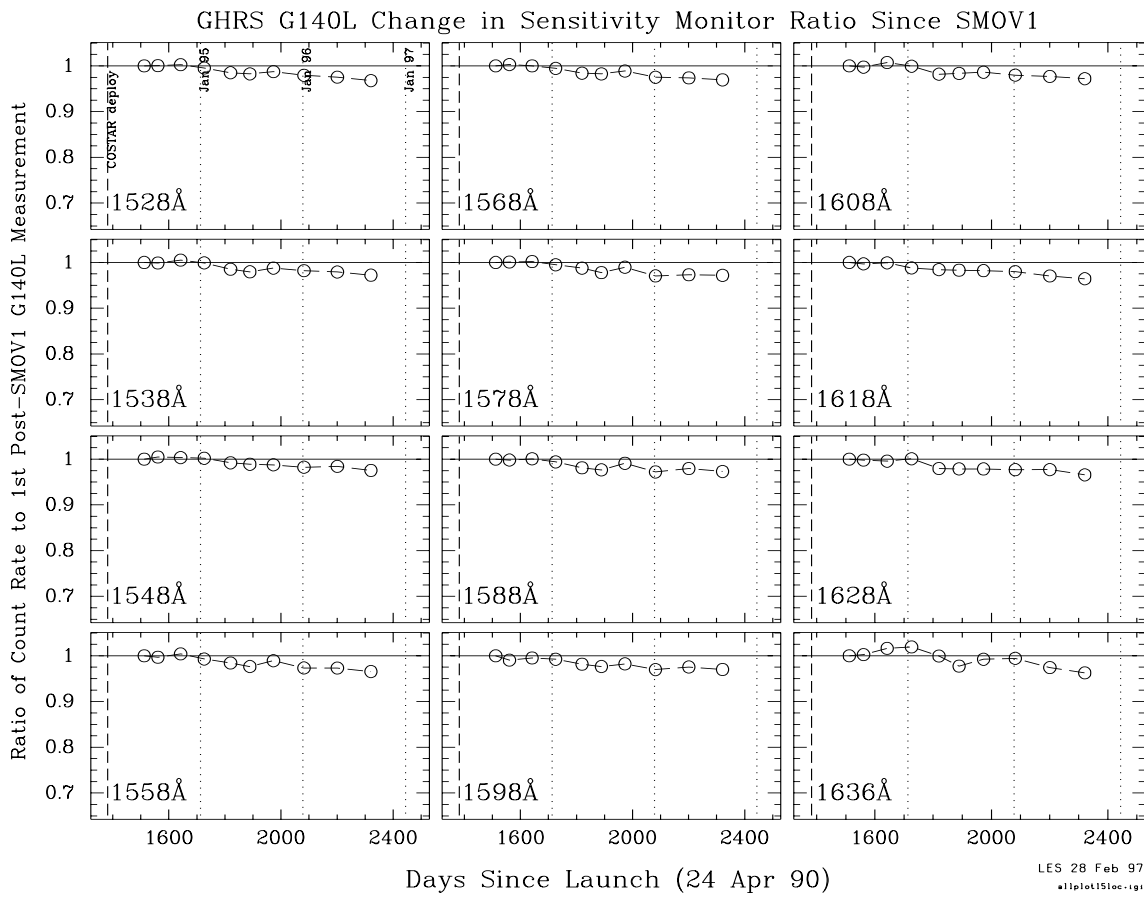
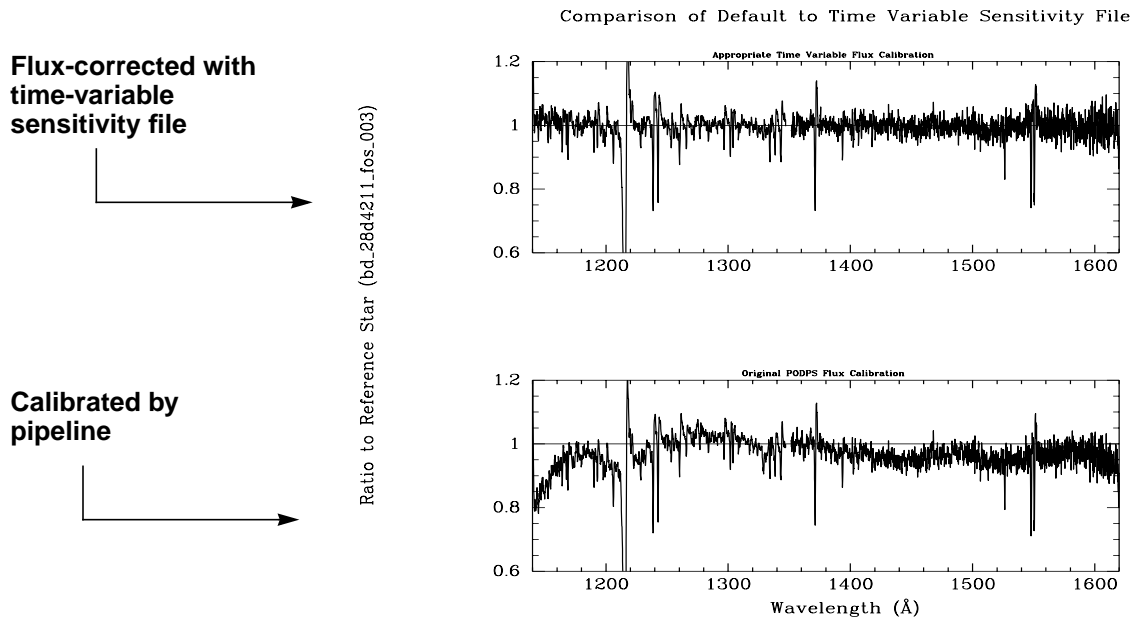


Figure 37.6: Ratio of Monitor Data to Reference Star



37.2.4 Calibrated Flux Quality

Absolute and Relative Fluxes

The foregoing discussion of the process used to create the components of the flux calibration illustrates some of the factors that influence the quality and reproducibility of flux calibrations in GHRS observations. You want to know how precise and accurate the flux values are, and that varies by situation.

For example, if the same point-source object was observed repeatedly at the same wavelength with the same grating, then many variables are removed. This situation is essentially that for BD+28 in the monitoring program. Figure 37.3, for example, shows that once the long-term trends are removed, Side 2 LSA fluxes for this best-case scenario are reproducible to within about 1%. The primary source of this uncertainty is error in positioning a star in the LSA. The uncertainty with the SSA will be significantly larger because the throughput of the SSA depends critically on centering the star, while the LSA is much less sensitive to that.

Now suppose that the same instrumental setup is used throughout (grating and wavelength do not change) but that different stars are being compared. If the stars have similar spectra, then the previous situation pertains. If the spectra differ significantly, then the convolution of that spectrum with the sensitivity and vignetting functions will introduce additional uncertainty. Near the center of the spectrum these effects will be minimal and the intercomparability should be to within 1 to 2%.

The same kind of additional uncertainty arises if the same or different objects are being compared but in a situation where the grating used or central wavelength are different. For example, one star may have been observed with G140L and the other with G140M, or perhaps G140L was used for both, but at different settings. In this instance some of the shape effects we described will apply—in the worst cases there can be uncertainty of about 4%, but 2 to 3% is more typical.

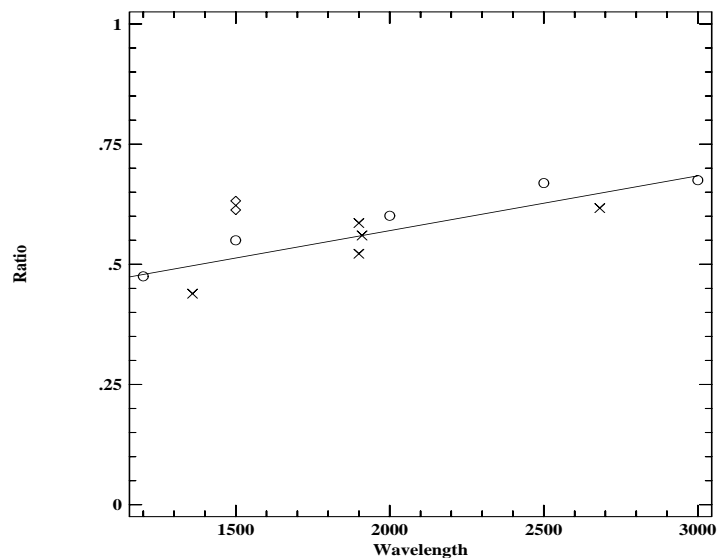
In other cases, you might want to know the quality of the flux on an absolute basis, perhaps to compare to models. This uncertainty is impossible to measure fully, but a comparison of observations from different instruments at different times indicates that fluxes on an absolute scale are reliable to about 5%. The absolute flux scale used by the GHRS is tied to the system of STScI observatory standards. In May 1994, we switched over to the new, revised absolute flux scale established from observations of the white dwarf G191-B2B (see *GHRS ISR 062*). The new scale differs from the old by up to 10%, depending on wavelength. Archived data obtained prior to May 1994 have not been recalibrated with the new flux scale. Therefore, spectra of the same star *calibrated* before and after May 1994 are on fundamentally different flux scales; recalibrating pre-May 1994 data with the latest GHRS reference files will produce calibrated data on the white dwarf flux scale. Bohlin et al. have compared FOS observations of white dwarfs to models and find consistency to within 2%. They also estimate that various systematic effects may lead to an overall error in absolute fluxes of about 5%, as we noted, but these errors are common to all the systems, meaning that the uncertainty with which HST fluxes can be compared to, say, IUE fluxes, is much lower and is comparable to comparing just HST fluxes.

The absolute throughput of the LSA is not well known. We estimate, based on models of the point spread function, that approximately 90 to 95% of the light of a point source that reaches the GHRS focal plane is encompassed by the LSA.

The relative throughput of the SSA with respect to the LSA was determined before and after the installation of COSTAR (see *GHRS ISR 062*). Post-COSTAR values are shown in Figure 37.7. LSA throughput is assumed to be 100% in this figure. The relative throughput of the SSA is wavelength dependent, with higher values measured at longer wavelengths. The pipeline automatically corrects for the point source differential aperture throughput.

In Figure 37.7, the circles are observations of μ Col—all five data points are based on a single SSA ACQ/PEAKUP. The crosses are for χ Lup; the first and last points are from a single ACQ/PEAKUP and the cluster of three points near 1950 Å is from another. The diamonds are for AGK+81D266; each point is based on an individual ACQ/PEAKUP. The solid line is a straight line fit to the μ Col and χ Lup data.

Figure 37.7: Ratio of Count Rates for Post-COSTAR SSA to LSA



Sensitivity Changes Over Time-Scales of Months to Years

We noted earlier the evidence for changes in GHRS sensitivity with time since the first servicing mission. Corrections for the effects of these changes have been incorporated into CDBS so that you should get back the appropriate sensitivity reference file for the time an individual observation was taken.

Side 1

The largest effects are seen for grating G140L, especially below Lyman- α . From the monitoring data, a ratio and errors were calculated every 10 Å from ~1100 Å to ~1630 Å. While the sensitivity below Lyman- α decreased, an apparent increase occurred in sensitivity from ~1200 to 1350 Å, before it declined again. We do not understand this behavior, but it has remained fairly constant with

time. In addition to rederiving the baseline post-COSTAR G140L sensitivity, we have also created time-dependent G140L curves for the date of each sensitivity monitor based on the ratio of the counts from the monitor to the SMOV baseline data. Observers will need to interpolate between sensitivity curves to get a correction appropriate for the date of their observations. The derivation of these Side 1 changes is described in *GHRIS ISR 085*.

Side 2

The results of the Side 2 GHRIS medium-resolution sensitivity monitor suggest that since COSTAR was installed, the GHRIS sensitivity changes between 1200 Å and 3000 Å do not exceed about 5%. We find evidence for a time-dependence of the sensitivity with a decline rate of about 2% per year. As an example we showed in Figure. 37.3 count rate ratios of BD+28D4211 obtained since COSTAR installation, focus, and alignment and referenced to the beginning of Cycle 4. (Details for the Cycle 4 observations are in *GHRIS ISR 071*). *The sensitivity files used by calhrs reflect the state at the beginning of Cycle 4. The changes seen for Side 2 are described in GHRIS ISR 089.*

Note that the calibrated science data in the .c1h file take into account the different throughput for point sources of the LSA and SSA before and after the installation of COSTAR. Therefore a star observed before and after the installation of COSTAR will have the same flux although its count rate will be lower before COSTAR.

Decreasing Counts During an Orbit

A series of short-exposure spectra of a star over many orbits in ACCUM mode appeared to show a regular decline of the observed counts of roughly 10% over the course of each orbit. This is described in *GHRIS ISR 073*, together with some possible explanations. The best guess is that this phenomenon is due to telescope “breathing.” This effect can contribute to flux uncertainty, obviously.

Correction for Extended Sources

When **calhrs** photometrically calibrates your observations, it assumes you have observed a point source, and adjusts the flux in your spectrum to account for light loss due to the PSF outside of the aperture, i.e., it returns the flux you would have seen if all of the flux from your point source fell within the aperture. Therefore, the absolute fluxes of point sources measured through the LSA and SSA should be the same. Of course, the count rates will be lower for the SSA observation but **calhrs** will automatically apply a different sensitivity function to the SSA observation to account for the light loss. The properties of the GHRIS apertures are presented in Table 37.3.

calhrs always assumes a point source is observed and it effectively applies a correction factor for the light lost outside the aperture. If you observed an extended source, then your source does not fill the aperture as does a point source and the flux calibration from **calhrs** will be inappropriate. To obtain a rough estimate of the specific intensity multiply the observed flux by 0.95 ± 0.02 for observations taken through the LSA and divide by the area of the aperture in square arcseconds. This assumes that the extended source completely and evenly fills the

aperture. For pre-COSTAR observations, the correction factor is 0.725 (see *GHRIS ISR 061* for details).



The absolute fluxes for extended sources obtained with **calhrs** are incorrect.

Table 37.3: Properties of GHRIS Apertures

Name	Clear Aperture (mm)	Pre-COSTAR	Post-COSTAR	Shape
LSA	0.559	2.0 arcsec	1.74 arcsec	square
SSA	0.067	0.25 arcsec	0.22 arcsec	square

Correction for Background Counts

The background level, or dark current for both GHRIS detectors was very low: typically about 0.01 counts per second per diode when well away from the South Atlantic Anomaly. However, for very faint objects the dark level could dominate the signal, and accurate correction for the background is vital.

Because of this, some provision was made in the GHRIS commanding software for features that would allow for lower net noise rates compared to standard observing modes. One of these modes used the CENSOR option, and the other used a parameter called FLYLIM. These will not be detailed here as they were rarely used. They are described in the *GHRIS Instrument Handbook*.

For archival data there are several options for correcting for background. These were described in the previous chapter (see “Calibration Steps Explained” on page 36-2). Investigate this issue carefully before choosing the method, especially if your target was faint. You may wish to consider how many counts were collected in the background spectra that were obtained as part of the stepping pattern, for example, and to see if your object was observed in the vicinity of the SAA. *GHRIS ISR 070* discusses measurements of the background for Side 2 in detail, and *GHRIS ISR 085* describes the model used for estimating background counts.

37.3 Spectrum Shape

The shape of the spectrum and its overall level are closely tied, which is why both sensitivity and vignetting were discussed in the previous section. Here we go into vignetting and related effects a little further.

Shape Effects from the Sensitivity Function: G140L

For most GHRIS observations, the observed bandpass samples only a small portion of the spectrum produced by a grating. Therefore, undulations in the sen-

sitivity function, which have length scales of many Ångstroms, at most have a small linear effect across a given spectrum.

G140L is an exception to this rule because it produces spectra nearly 300 Å long. Spectra from grating G140L may have modest shape effects that have their origin in the sensitivity function. These can be especially pernicious near Lyman- α because the breadth of that feature in the standard stars we observed prevented a good determination of the shape of the underlying sensitivity function at those wavelengths.

Light Falling Off the Diode Array

Thermal drifts caused a spectrum to move on the photocathode, so the GHRs routinely performed a SPYBAL (spectrum Y-balance) to properly center the spectrum on the diode array. A SPYBAL was performed every time a new spectrum element was used (i.e., the first use of a different grating) and approximately every two orbits thereafter. This centering can be important because a given spectrum is tilted across the diode array, and lack of proper centering could result in the ends of the spectrum falling off the array. Again, this is routinely corrected for and only becomes a problem if SPYBALs were suppressed for long exposures (i.e., several orbits).

A simple calculation can give us some idea of how large this effect can be. For example, the G140L spectrum of a point source may fall off the diode array due to drift as the temperature changes. Ignoring the width of the spectrum (something on the order of the size of the SSA or about 8 deflection units) the ends of the spectrum will differ by about 45 deflection units and will be within about 9 deflection units of the edge of the diode array. If we assume a worst case drift of about 25 deflection units (seen over 10 hours), we find that at the end of this time about 25% of the spectrum will have fallen off the edge of the diode array!

In the case of an extended object uniformly filling the LSA, the effect is much more pronounced. In this case the width of the spectrum cannot be ignored. The width is equal to the size of the aperture or about 64 deflection units. For the case of a G140L observation of an extended object in the LSA, we start out with a loss of light. The spectrum is already falling off the array with the ends experiencing about 30% light loss. In the time it takes to drift 25 deflection units, some part or all of the spectrum may fall off the array, resulting in a significant reduction in signal.

G270M Vignetting Errors

The pre-COSTAR, in-flight sensitivity calibration for this grating is wrong shortward of 2300Å for the period November 11, 1991 through April 1, 1994. The pre-COSTAR vignetting correction for grating G270M is inadequate shortward of 2300 Å, and the post-COSTAR vignetting correction shortward of about 2150 Å is not handled properly by *calhrs* because the Y-deflection has not been measured below 2300 Å. The program which was to correct this failed. Please see *GHRs ISR 077* if you wish to analyze data taken during this time period with this vignetting.

The Echelle Blaze Function

The echelle blaze function relates relative fluxes to those observed at the center of a given spectral order. This function was determined by observing the standard star μ Col at a number of different wavelengths in different orders, and relating those observations to others made with first-order gratings. It was impossible to cover fully a free spectra range or to sample every echelle order, so the blaze function is meant to be a reasonable approximation to the true function. An underlying, but unstated, assumption, is that observers used the echelles to measure the strengths or positions of weak spectrum features and were therefore not primarily concerned about the absolute flux level in the final, reduced spectrum.

Inappropriate Background Subtraction

In some cases the shape of a spectrum can be distorted if the background is improperly calculated and subtracted. This was seen in the first couple of years of GHRS operation because the background subtraction software fitted a polynomial to the background before subtracting it from the source spectrum. This was done to preserve shape in the background spectrum, but often the background had very few counts so that the fit was spurious. Modification of the procedure to fit a flat line removed the problem.

37.4 Spectrum Noise and Structure

Dead or Noisy Diodes

Each diode of the linear array (containing 512 diodes, diodes 7–506 are science diodes) was independently monitored via its own electronics chain. Diodes could exhibit anomalous behavior or fail. These diodes were grouped together as *dead* or *noisy* diodes. Diodes that showed anomalous behavior over an extended time were turned off for science observations. In practice, the threshold voltage for anomalous diode was set to a high value so that it did not detect electrons from the photocathode. The GHRS calibration software corrects for known anomalous diodes. If anomalous absorption features are present in the calibrated data, new noisy or dead diodes may be at fault. The non-standard thresholds for detector diodes are listed in Table 37.4.

Table 37.4: Problematic or Otherwise Important GHRS Diodes

Science Diode # ^a	Diode # 1-512 ^b	AMP/CH ^c	Threshold ^d	Comments
<i>Detector (Side) 1</i>				
	1	24/07	46	Large background diode (50% peak +3)
	2	24/08	44	Large background diode (50% +3)
	3	27/07	120	Gold coat radiation diode
	4	00/08	255	Diode not connected by design

Table 37.4: Problematic or Otherwise Important GHRS Diodes (Continued)

Science Diode # ^a	Diode # 1-512 ^b	AMP/CH ^c	Threshold ^d	Comments
85	91	30/00		Dead—BDT ^e r0h, r5h change May 29, 1995 (95149 SMS)
123	129	22/05	50	Threshold 60% stops noise
262	268	15/12	255	Dead electronics—in BDT
273	279	11/04	255	Bad contact—crosstalk when contact made. In crosstalk table
436	442	00/15	52	Threshold 60% stops noise
445	451	00/03	44	Bad 4096 bit—in bad diode table (BDT)
487	493	08/07	255	Very noisy—in BDT
	510	04/08	120	Gold coat radiation diode—not functional
	511	04/07	42	Large background diode (50% peak +3)
	512	08/08	47	Large background diode (50% +3)
Detector (Side) 2				
	1	24/07	46	Large background diode (50% +2)
	2	24/08	44	Large background diode (50% +2)
	3	27/07	120	Gold coat radiation diode
	4	00/08	255	Diode not connected by design
51	57	25/05	255	Bad diode—added to BDT 26 Feb 96.
80	86	30/14		Threshold 60% stops noise April 20, 1992, r0h
104	110	27/11	255	Bad diode—in BDT
140	146	24/13	40	Threshold 80%, crosstalk noise
144	150	25/12	255	Bad diode in BDT
146	152	16/09	49	Threshold 50%, occasionally noisy
168	174	24/10	43	Threshold 50%
237	243	16/00	44	Threshold 50% April 20, 1992; threshold 100% May 15, 1995
263	269			Flaky: intermittently strong (see <i>GHRS ISR</i> 080).
273	279	11/04	255	Bad contact—crosstalk April 20, 1992
293	299			Flaky: intermittently weak (see <i>GHRS ISR</i> 080).
313	319			Flaky: intermittently strong (see <i>GHRS ISR</i> 080).
339	345			Flaky: intermittently weak (see <i>GHRS ISR</i> 080).
342	348	11/10		Threshold 100% April 20, 1992
355	361			Flaky: intermittently weak (see <i>GHRS ISR</i> 080).
423	429			Flaky: intermittently weak (see <i>GHRS ISR</i> 080).

Table 37.4: Problematic or Otherwise Important GHRS Diodes (Continued)

Science Diode # ^a	Diode # 1-512 ^b	AMP/CH ^c	Threshold ^d	Comments
426	432			Flaky: intermittently weak (see <i>GHRS ISR</i> 080).
440	446	00/14	41	Threshold 50%
441	447	01/02		Threshold 70% April 20, 1992
442	448	02/13	44	Bad 16384 bit—in bad diode table
	510	04/08	120	Gold coat radiation diode
	511	04/07	43	Large background diode (50% peak +2)
	512	08/08	41	Large background diode (50% peak +2)

a. Science Diode: diodes 7–506 used for science observations.

b. Diode: the entire (1–512) diode array.

c. AMP/CH: Amplifier/channel, onboard electronic location of diode.

d. Threshold: Discriminator threshold voltage setting for channel.

e. BDT: Bad diode table.

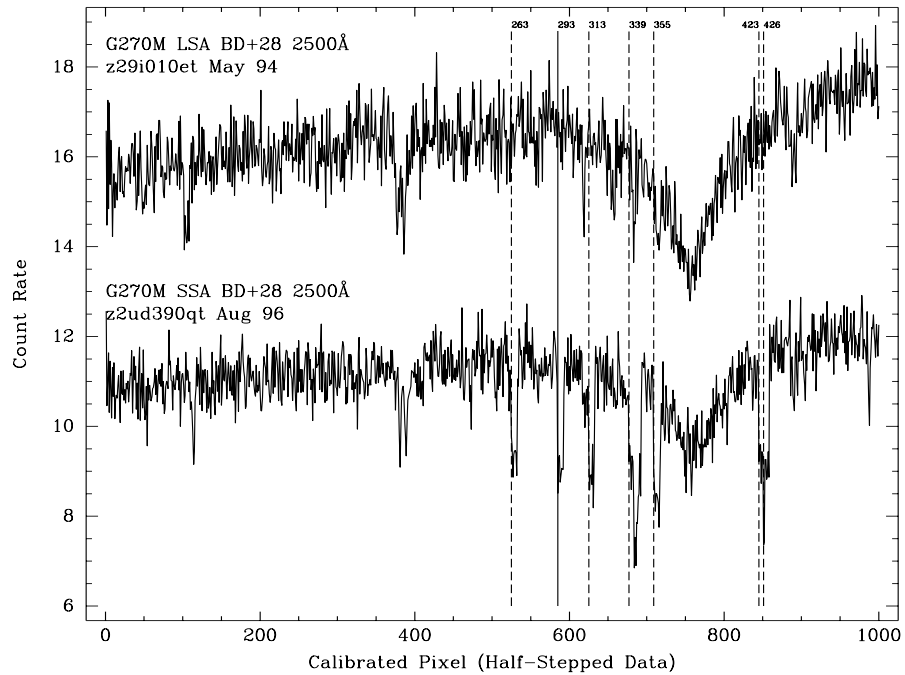
The easiest way to tell a bad diode from an absorption line or blemish is by the width, flat profile, and location. The width will depend on your comb addition, sub-stepping strategy (see “File Sizes” on page 35-5), and which file you are in. Dead diodes in data taken with the default comb addition will be 4-pixels wide in raw data and 16-pixels wide in default (quarter-stepped, merged) calibrated data. Dead or flaky diodes will be generally flatter than an absorption line. A dead diode, in raw data, is illustrated in Figure 37.9.

Flaky Diodes

In 1996 we noticed, first in some Side 2 CVZ RAPID mode data, that there were anomalous absorptions (so-called *flaky diodes*) in the data. Eventually we determined that increases in the GHRS pre-amp temperature resulted in non-linear amplification of input charge from diodes, effectively resulting in the occasional appearance of flaky diodes in spectra, as if a change in the threshold voltage had changed the response of a few Side 2 diodes. This phenomenon, also apparent in non-CVZ data as GHRS usage become heavier, is discussed in more detail in *GHRS ISR* 78. The same effect was *not* noticed in Side 1 spectra. Table 37.4 lists diodes that are occasionally seen as flaky in data after 1996. If you think you have seen flaky diodes, check the width of the features and which pixels are affected. The first low raw pixel in each feature should agree with the science diode value in Table 37.4 above.

Blemishes

Scratches, pits, and other microscopic imperfections in the detector window and on the photocathode surface are referred to as *blemishes*. The magnitude of blemishes upon spectra depends on how the spectrum illuminates the photocathode near a blemish. Many blemishes have spatial structures and depths that would make them difficult to distinguish from real stellar or interstellar features, see Figure 37.9. Therefore, it is difficult to automatically correct data for the effect of

Figure 37.8: Side 2 Diodes that Become Flaky at High Temperatures

blemishes. In the absence of independent information, individual subexposures can be displayed in diode space to identify non-real spectral features. The calibration code does not correct for blemishes. However, the data quality file (.cqh) contains data quality values marking which pixels are affected by known blemishes. See Table 37.10 for information about data quality flags.

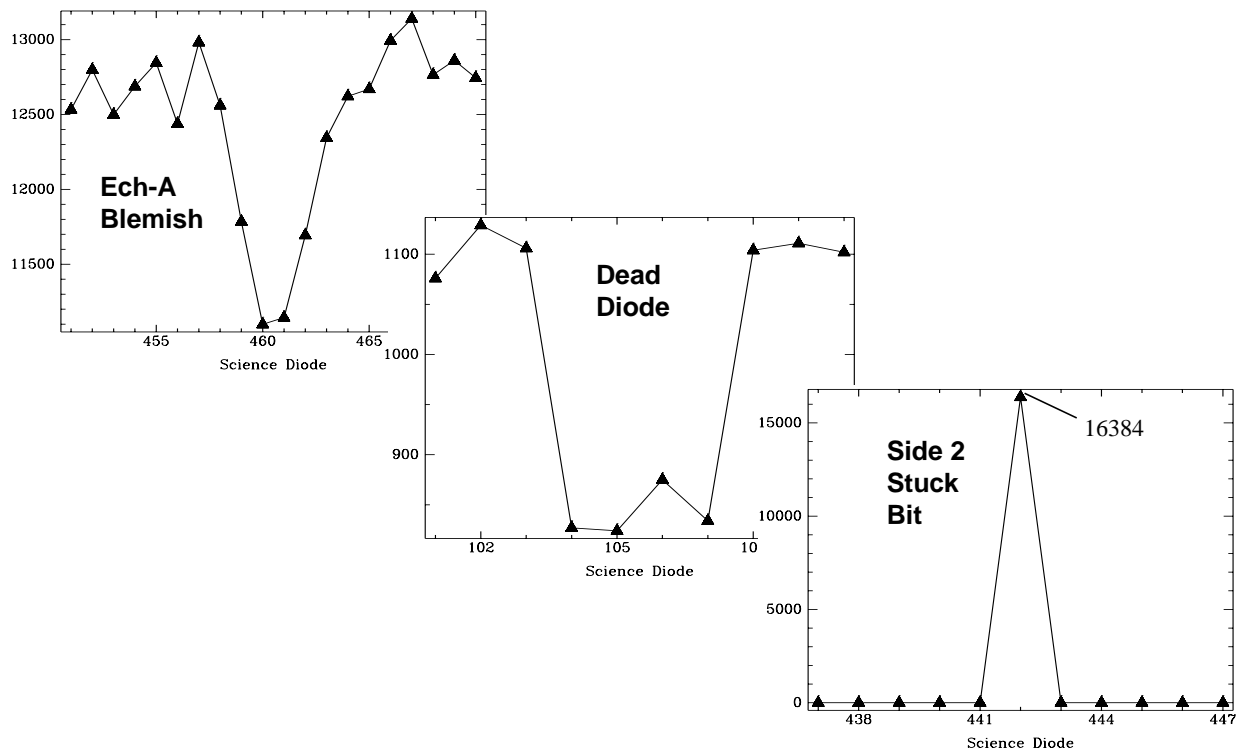
Spikes

Large spikes and unrealistic flux levels were found in a subset of Fall 1995 calibrated GHRS data. The affected observations were all made using the Ech-A grating in orders 35 and 36. Fortunately, this problem only affects a handful of observations in a few proposals. The solution to the problem is to recalibrate with a vignetting file with the groups in ascending line position order (e.g., `fc11607fz.r2h`, or more recent).

Also the stuck bit at Side 2 science diode position 442 will look like a spike as shown in Figure 37.9.

Granularity

As we noted in the previous chapter, the first-order diode-to-diode response variations are removed in `calhrs`. There are also granularity effects produced in the photocathode faceplates of the detectors. No calibration is provided for these because determining them is impractical. However, grating G140L has been so characterized because its bandpass is large (see *GHRS ISR 076* for details on how this was derived). For the other gratings, features such as FP-SPLIT and COMB addition were provided to allow for improved signal to noise in the final spectrum.

Figure 37.9: Sample Blemish, Dead Diode, and Stuck Bit

37.5 Calibration Quality Files

calhrs reads the raw data quality files, operates on the data using the quality flags as a discriminate, and flags the appropriate data values in the output quality files. Fill data are ignored. Reed-Solomon flagged data are calibrated, but is flagged as suspect in the output quality files.

The initial error in the data is assumed to be Poisson-limited. The error is propagated mathematically through the calibration process. The propagated statistical error file (.c2h) contains a measure of the statistical errors of the original data values; this file is calibrated in lock-step with the science data files.

The flux data quality file (.cqh) flags bad pixel values in the calibrated flux and propagated statistical error files.

Special diodes data quality files (.c4h) flags bad pixel values in the calibrated special diodes file (.c3h). Good pixel values are identified by a zero value.

Table 37.5: Calibrated Data Quality Flags

Flag Value	Description
Category 1: Data not useful—data values set to zero	
800	Data filled
400	Dead or disabled channel
300	Severe saturation (uncertainty >50%)
Category 2: Data uncertain—uncertainty not indicated in error computation	
190	Large saturation correction (uncertainty > 20%)
180	Photocathode blemish (deep)
150	Photocathode blemish (medium)
140	Photocathode blemish (small)
130	Moderate saturation correction (uncertainty >5%)
100	Reed-Solomon decoding error
Category 3: Data uncertain—uncertainty indicated in propagated error file	
30	Dead diode contributed to comb-added data point

37.6 About Wavelength Calibrations

37.6.1 Aperture Offsets

By convention all GHR wavelengths are referred to the SSA. Corrections to apparent wavelengths from sources in other apertures is necessary because light from those other apertures enters the GHR at angles slightly different from that of the SSA. These corrections are called *aperture offsets*.

During calibration, the zero-points of the wavelength scale are adjusted for the difference in incidence angle of apertures LSA, SC1, and SC2 from the SSA. Incident angle correction (IAC_CORR) coefficients are found in the CCR8 table. Currently, an average value for the zero-point wavelength correction is applied to all first order grating LSA observations regardless of the carousel position. The recently-calculated and old offsets for GHR gratings are listed in Table 37.6, which is taken from *GHR ISR 080*. These coefficients are used to compute the offset using the following formula:

$$\lambda = \lambda + (A + Bs)/m$$

where:

- λ is the wavelength.

- A and B are coefficients from `ccr8`.
- s is the photocathode sample position.
- m is the spectral order.

Table 37.6: Incident Angle Correction for GHRS Gratings

Grating	A	B	Previous A
G140L	0.0	0.0	0.0
G140M	-0.0065	0.0	0.0
G160M	-0.0448	0.0	-0.022±0.023
G200M	-0.057	0.0	-0.037±0.012
G270M	-0.060	0.0	-0.036±0.007
Ech-A	$-0.0076 \times m$	0.0	0.0
Ech-B	$-0.0078 \times m$	0.0	0.0

37.6.2 Doppler Compensation

Since HST orbits the Earth with a velocity of 7.5 km s^{-1} , spectra obtained with GHRS could see a Doppler shift of up to 15 km s^{-1} . The effect of the spacecraft velocity was corrected for in real time for ACCUM mode observations by deflecting the image of the spectrum an amount equal to the Doppler shift so that the spectrum appears fixed with respect to the diode array which is recording the spectrum. RAPID mode observations are not corrected for this effect. Unfortunately, it was discovered that GHRS spectra obtained prior to the end of March 1993 suffered from incorrect Doppler compensation.

The problem became visible in a set of high dispersion spectra obtained with short exposure times, where one could actually see a doubling of spectral features corresponding to the different Doppler shifts applied. At the maximum required correction, the flight software was mistakenly applying zero correction. Affected data will be obvious only in extreme cases, but the problem may degrade your data even when the effect is not obvious.

An on-board fix to the first problem was implemented in the flight software as of April 1993. Observations made after the update should not suffer from the Doppler compensation error. However a cumulative error in the onboard Doppler compensation still existed, which caused the accuracy of the Doppler compensation to be reduced for long exposures.

The `obsum` task in the STSDAS `calhrs` package can be used to identify GHRS spectra which were potentially corrupted by the first Doppler compensation problem. This task identifies periods when the Doppler compensation should have

been maximal and provides information to allow you to estimate the fraction of the data in each group that is contaminated by incorrect Doppler compensation. If a substantial fraction of the data are corrupted for a given period of time, the only recourse is to discard the affected groups and reduce the remaining good data. See the help file of **obsum** for a detailed description of its use.

Also, all observations of moving targets made before July, 1994, were compensated incorrectly. The fix to this problem was implemented in July 1994 and moving target observations since then do not exhibit that problem. For help identifying and correcting moving target observations, please contact the STScI Help Desk via E-mail to help@stsci.edu.

37.6.3 Geomagnetically Induced Motion

The displacement of the image relative to the diodes due to the earth's magnetic field, Geomagnetic Image Motion (GIM) problem, may affect a GHRS observation depending upon the length of the exposure and the orbit during the observation. The rate of drift of an image across the diodes was small enough that there is no significant smearing of data on time scales of five minutes or less. Very long exposures may exhibit GIM related symptoms and should be investigated by the user. No correction for GIM has been incorporated into either the operations of the GHRS or in the data reduction procedures.

37.6.4 Carrousel Properties

The carrousel was rotated to engage the desired dispersive element or mirror and to place the requested wavelength at the center of the diode array. In the spring of 1991, the Side 1 carrousel control electronics developed an intermittent failure and the carrousel function was modified to operate the Side 1 carrousel from the Side 2 electronics. Any Side 1 observation obtained after April 1991 will have different carrousel function coefficients for specific wavelengths.

During normal operation, the carrousel was commanded to rotate to a pre-selected position depending upon the carrousel function. The carrousel could oscillate before achieving the desired position and take an appreciable amount of time to lock at that position. This may take longer than the normal amount of allocated time and thereby, following observations are affected. Before Spring 1995, if the carrousel took a significant time to lock, the following observations would not occur and be lost. After spring 1995, the flight software was updated to *time out* a set of GHRS observations if the end time of the observations was reached. The time-out was not enforced for GHRS target acquisitions. The header keyword FINCODE (see Table 37.7) will be set to 106 to indicate to the observer that a time-out occurred. The affected GHRS observation may be several observations down stream of the observation for which the carrousel took too long to lock into position. The STSDAS task **obsum** in the **calhrs** package can be used to display to the screen the carrousel position and the FINCODE values.

```
st> obsum z2bd010c
```

Table 37.7: GHRM FINCODE Values

FINCODE	Explanation	Action
15	X-null balance failure during coarse locate	Usually benign
16	X-null balance failure during fine locate	Usually benign
20	Number of slews to center exceeded max	Usually benign
101	Normal beginning of observation	-
102	Normal end of observation	-
104	Observation ended, over-exposure	Exposure may have been shortened
105	Observation ended, too many bad data	Exposure may have been shortened
106	Observation ended, time out	Exposure may have been shortened

37.6.5 Wavelength Data Quality

The pipeline data reduction system (PODPS) automatically assigns a wavelength scale to your GHRM ACCUMs³ and RAPIDs when they are reduced. Note that this default wavelength scale is the one appearing in the .c0h file that goes with the .c1h file containing fluxes, *even if there is a wavelength calibration exposure (wavecal) available for that program*. If you have a wavecal, you must analyze it and apply the results yourself; this is explained in the section “Recalibrating GHRM Data” on page 36-13.

This default wavelength scale is calculated using terms that depend primarily on the carrousel position (i.e., the orientation of the grating that was used), but there are also terms for the temperature within the GHRM (recorded in the engineering data stream). There is also a weak time-dependent term.

The default wavelength scale is good to approximately one diode rms, with contributions from various effects as enumerated in Table 37.8 (which is taken from Heap et al., 1995, *PASP*, 107, 871). Not listed is the error in wavelength that occurs for observations made in the Large Science Aperture (LSA), which was discussed in “Aperture Offsets” on page 37-23.

3. Here and elsewhere in this chapter we will consider OSCANs and WSCANs as equivalent to ACCUMs. Both OSCANs and WSCANs are macros that generate a series of ACCUMs when the program is executed on the telescope.

Table 37.8: Wavelength Error Sources

Source of Error	Maximum Error (diodes)
Quality of dispersion coefficients	0.1
Incident angle correction, SC2 to SSA	0.1
Uncertainty in thermal and time models	1.0
Short-term thermal motions	0.4 hour ⁻¹
Carrousel repeatability	0.5 (0.17 typical)
Onboard Doppler compensation effects	0.15 typical
Geomagnetic image motion	0.25
Uncertainty in centering target in SSA	0.21

The largest sources of uncertainty in wavelength are obviously due to the geomagnetic image motion (GIM) and the model used to correct for thermal and time effects. We cautioned observers to break down long exposures into units lasting no more than five to ten minutes, in order to reduce the effects of GIM below significant levels. Thus you should not ordinarily find GIM leading to loss of resolution in the final spectrum.

Thermal effects, however, include a significant component that appears to be unpredictable. These thermal effects are best removed through use of a wavecal or SPYBAL. Thermal motions are just that: a motion of the overall image of the spectrum. The changes in image scale—dispersion—that occur are very small and can safely be ignored in most instances. For example, for grating G270M, the centers of our calibration spectra deviate from the default wavelength scale by no more than 100 mÅ (and typically about 70). The slope of a fit through the measured positions for the comparison lines relative to the default wavelength scale deviates in the center by no more than 100 mÅ (and typically about 70 mÅ), and has a slope of about 3×10^{-4} (in dimensionless units of Å per Å), so that the ends deviate from the center by, typically, about 3 mÅ across a 40 Å wide spectrum. The rms scatter of the fit is typically about 0.2 km s⁻¹. Not all the gratings are this good, and some other values for the quality of fit are provided in Table 37.9. The data in that table are taken from *GHRS ISR 081*, which summarizes wavelength calibrations for the first-order gratings in Cycles 4, 5, and 6 (i.e., post-COSTAR). Other ISRs with wavelength analyses include:

- *GHRS ISR 035*: An analysis of Side 2 data in 1990 and 1991.
- *GHRS ISR 039*: A check on the accuracy and repeatability for the pipeline wavelength calibrations after dispersion tables were corrected in 1992.
- *GHRS ISR 052*: An assessment of pipeline calibrations for the first-order gratings on Side 2 in Cycle 2.
- *GHRS ISR 058*: An assessment of pipeline calibrations for Echelle-B in Cycles 2 and 3.

Table 37.9: Quality of Default Wavelength Scale for Side 2 First-Order Gratings

Grating	rms deviation of fit(mÅ)	Deviation at center (mÅ)	Slope of fit (times 10 ⁴)
G160M	7 to 11	60	0.2
G200M	30 to 50	20 to 80	0.2
G270M	7 to 16	50 to 100	0.3 to 0.5

37.7 Spatial Uncertainty: Target Acquisition Problems

Most of this topic was discussed in the chapter on data assessment and in *GHRS ISR 079*, “Interpreting GHRS Target Positioning”. An onboard target Acquisition performed a spiral search followed by returning to the dwell point with the most counts. The end phase of the onboard acquisition was the locate phase (coarse y and x centering with a fine x balance at the end of the locate phase).

GHRS target acquisitions of very bright stellar targets could fail during the locate phase. This resulted from low contrast between the central four diodes of the eight diodes used for acquisitions. The high count rate in the central four diodes flattened the point spread function (PSF) leading to wrong centering in the aperture. The SSA science observations in this case may contain just noise.

The header keyword FINCODE value indicates the success or failure of the GHRS observation. FINCODE=102 indicates the observation completed successfully as planned, but does not indicate whether the target was centered in the aperture. Any other value for FINCODE indicates a possible problem. During RSDP pipeline calibration, if a FINCODE value is encountered other than 102, a warning message is written to the trailer file (.tr1).

From April 1989 through August 1994, OSS (now part of OPUS) created an Observation Comment file (extension .ocx) for every HST observation. After that time through January 1995, OSS created an .ocx file for degraded observations. If an .ocx file exists for an observation, it should be checked for anomalies. (See Chapter 38 for more information.)

If OMS observation logs were created for an observation, they should be checked to verify that no anomalies occurred during the target acquisition.

Low Count Rate

Observations with low count rates, containing mostly noise, may contain few detected or no counts from the target. Calibrated data may have a bell or U-shaped appearance, quantized data values, or extremely low flux values. These data indicate a missed target, a target too faint for the GHRS, or inappropriate use of the GHRS.

37.8 Observation Timing

Knowledge of the exact time that observational activities take place onboard GHRS is not directly available. Instead, we only get timing information when data are dumped to the ground from the onboard computer from which we may infer when things happened. When data are dumped they are given time tags from the NSSC-1 computer; the spacecraft clock has a time resolution of approximately 0.125 seconds. While GHRS can operate on shorter time scales (0.050 seconds), information about these activities does not make it into the telemetry stream.

Nevertheless, as an observer, you may want answers to the timing questions posed in this section. You may find the `hst_calib.observ` task helpful in determining timing questions.

37.8.1 When Did the Observation Start?

The closest time tag to the start of most exposures (excepting RAPIDs) is the packet time (PKTTIME) on the first group of the Unique Data Log (UDL), which is the data file with the `.u1h` extension (see the discussion on data structure in “Contents of Delivered Data” on page 35-1). A UDL is always dumped from the spacecraft prior to the start of a science exposure, effectively flagging the start of the observation. The PKTTIME keyword holds an MJD value good to a spacecraft clock tick (~0.125 sec). This MJD value (for ACCUM mode observations) is stored in the EXPSTART keyword in the science data headers (`*.d0h`, `*.c1h`). The accuracy of the start time is limited to the accuracy of the spacecraft clock—about 0.125 seconds.

For RAPID mode observations, the data are dumped as soon as they are taken. The PKTTIMEs represent the time the data left GHRS; calibrated data inherit the PKTTIMEs of the raw science data. The first two and last raw science packets (`*.d0h`) contain hysteresis information and are thrown away. This is why the calibrated data (`*.c1h`) will have three fewer groups than the raw science data. The best estimate of when a RAPID observation started is the PKTTIME of the first calibrated science packet (`*.c1h[1]`) *minus* the sample time of the observation, which, in this instance, can be found in the STEPTIME keyword. The accuracy in this case is half of a spacecraft clock tick (~0.0625 seconds). Unfortunately, the EXPSTART keyword in RAPID mode data appears to be incorrect.

37.8.2 When Did the Observation End?

For ACCUM mode observations, a second UDL is dumped at the end of the exposure and prior to reading out any science data. Therefore, the PKTTIME of the second group of the UDL can be used to mark the end of the exposure. For observations generating multiple readouts (e.g., FP-SPLITs and repeats) the UDLs come in pairs bracketing the science exposures. The MJD value of the second UDL in a pair should be used as the approximation of the ending of ACCUM mode observations. The accuracy is the same as the start time: about 0.125 sec-

onds. Misleadingly, the MJD value of the final * .d0h PKTTIME is placed in the EXPEND keyword.

For RAPID mode observations, a second UDL is not dumped until the last spectrum, which is a hysteresis measurement, has been dumped. In this case, the end of the observation is merely the time that the last spectrum has been read out and is contained in the PKTTIME for last group of the calibrated spectrum. Note that the PKTTIME for the science data is the tag when the science data are dumped and this must wait until the end of the exposure. Unfortunately, the EXPEND keyword for RAPID mode data is close to being the time-tag of the second UDL packet.

37.8.3 How Long Did the Observation Last?

The extent of an observation is reported in the EXPTIME keyword. This time may not be the same as the simple difference between the EXPEND and EXPSTART. (See “Was the Observation Interrupted?” on page 37-31.) The exposure time in the header is simply the exposure time you requested in your proposal times the number of exposures. To verify that you got the exposure time you expected you can calculate the EXPTIME using available header keywords as shown below.

ACCUM mode

$$\text{EXPTIME} = (\text{RPTOBS} + 1) \times (\text{fpsplits}) \times \text{MAXGSS} \times \text{INFOB} \times \text{STEPTIME}$$

where,

- RPTOBS = Number of exposures – 1 (i.e., the number of repeats).
- *fpsplits* = 1 (FP_SPLIT=DEF) or 2 (FP_SPLIT=TWO or DSTWO) or 4 (FP_SPLIT=FOUR or DSFOUR).
- MAXGSS and INFOB contain information concerning the STEPPATT and COMB used. If you want more details about these contact a GHRIS instrument scientist via the STScI Help Desk (help@stsci.edu).
- STEPTIME = the step time used (by default = 0.2 seconds).

RAPID mode

$$\text{EXPTIME} = (\text{groups}) \times \text{STEPTIME}$$

where:

- *groups* – is the number of spectra read out (i.e., the number of groups in the calibrated multi-group image, GCOUNT).
- *STEPTIME* – is the integration time for each spectrum (specified as SAMPLE-TIME in the proposal).

37.8.4 What was the Exposure Time Per Pixel?

The exposure per pixel is found in the EXPOSURE keyword in the calibrated flux header. This number is not equal to the EXPTIME because of the multiplicity of step pattern, FP-SPLITs and repeated observations.

This value is calculated by **calhrs** during pipeline calibration. To double check you may calculate EXPOSURE as follows:

$$\text{EXPOSURE} = \text{INFOC} \times \text{MAXGSS} \times (\text{STEPTIME} - 0.002)$$

where:

- INFOC and MAXGSS contain information about the STEPPATT and COMB used. (Note: INFOB and INFOC are different keywords containing similar information.)
- STEPTIME = the step time specified.
- 0.002 = the time in seconds of the internal overhead for integrating a single STEPTIME.

If you are interested in the exposure per diode, you must rebin the data from substep pixels to diodes.

37.8.5 Was the Observation Interrupted?

By design, the GHRs was interruptible: a given exposure may begin, be interrupted, and then resume. Observations were routinely interrupted for SAA passages and Earth occultations. The interruption could last anywhere from a few minutes, when skirting the SAA, to about half the orbit for an Earth occultation. In general, this is of no concern. Still, there may be times when you want to know the details of a given observation. Unfortunately, it is nearly impossible to determine when an observation was actually stopped and restarted—this information is just not available in the telemetry stream.

Additional details are available in the OMS observation log files as discussed in Appendix C of Volume I. It is also possible that a given observation may end prematurely. This information is encoded in the FINCODE keyword. We routinely see observations time out due to carousel resets. If you have additional questions about interruptions, contact the STScI Help Desk via E-mail to help@stsci.edu.

37.9 Instrument and Spacecraft Errors

All HST science observations are first received on the ground at White Sands, New Mexico, and are then relayed by satellite to the DCF (Data Capture Facility, after January 1996, PACCOR), Goddard Space Flight Center, Maryland. The DCF staff perform a check of the transmission using a Reed-Solomon error checking routine. When Reed-Solomon is used, the data are encrypted into a cyclic pattern.

The down-linked data are then decrypted and the Reed-Solomon code will verify the pattern and corrects, if possible, those words that are not as expected. If any packets are missing, DCF will wait for the next STR (space tape recorder) dump to verify no more data packets are forthcoming. Missing data packets and the results of the Reed-Solomon check are written to the data quality accounting capsule (QAC). The data packets and QAC are transmitted to the pipeline.

Each GHRS observation set was processed through the pipeline as far as generic conversion. The output of generic conversion is what users refers to as the *raw* uncalibrated dataset. Furthermore, the pipeline automatically ran the **calhrs** software to calibrate science files, such as ACCUMs, RAPIDS, and SPYBALs. Any ACQisition files, IMAGES, and DEFCALs are not calibrated.

Each science data file (.d0h), extracted data file (.x0h), and target acquisition (.d1h) have a corresponding data quality file containing flags or fill values for bad data. These quality files (.q0h,.xqh,.q1h) were created during pipeline processing and contain information extracted from the QAC or were filled during the data evaluation process. For each data point in the .d0h, .x0h, or .d1h file, there is a corresponding data point in the quality file. For each good data value, the corresponding point in the quality file is zero. If there are missing data (data-dropout), due to tape recorder flips, down link problems, or data loss due to unforeseen problems, the pipeline will pad the corresponding data file with fill data; the corresponding data point in the quality file was set to 16. If the data failed the Reed-Solomon error check, the corresponding data point in the quality file was set to one. Data that fails the Reed-Solomon check were classified as suspect, and may not be bad data.

Table 37.10: Pipeline Data Quality Values

Quality Value	Description
0	Good data point
1	Reed-Solomon error
16	Fill data